

An improved Parton Shower algorithm in QED

Carlo Michel Carloni Calame^{a,b}

^a*Dipartimento di Fisica Nucleare e Teorica, Università di Pavia*

^b*INFN, Sezione di Pavia*

Via A. Bassi, 6 - 27100 Pavia, Italy

Abstract

An improved QED Parton Shower algorithm to calculate photonic radiative corrections to QED processes at flavour factories is described. We consider the possibility of performing photon generation in order to take into account also the effects due to interference between initial and final state radiation. Comparisons with exact order α results are shown and commented.

Key words: Parton Shower, YFS, Event Generation

1 Introduction

The precise luminosity monitoring and data analysis at e^+e^- flavour factories (DAΦNE, PEP-II, KEKB) require that cross section calculations for QED final state processes ($e^+e^- \rightarrow e^+e^-$, $\mu^+\mu^-$, $\gamma\gamma$) have theoretical error below the 1% level. Also Monte Carlo simulations with the same accuracy are strongly demanded for data analysis. This implies to include the relevant radiative corrections, in particular the large effects due to multiple photon emission.

Aiming at providing a useful tool for data analysis, a Monte Carlo event generator (BABAYAGA) for QED processes at flavour factories has been developed. An exhaustive description of its main features and its basic theoretical ingredient, the QED Parton Shower (PS), can be found in [1]. Here, we remind only of the basics of the theoretical approach which the generator is based on, in order to describe recent improvements introduced in the code, aiming to give a more precise simulation also for exclusive radiative events. They concern the inclusion of the effects due to interference between initial state and final state radiation, which are not present in a pure PS framework.

2 The Parton Shower algorithm in QED

A widely used theoretical tool, to take into account the bulk of the photonic radiative corrections, consists in the calculation of the corrected cross section following the master formula [2]

$$\sigma(s) = \int dx_- dx_+ dy_- dy_+ \int d\Omega_{cm} D(x_-, Q^2) D(x_+, Q^2) \times D(y_-, Q^2) D(y_+, Q^2) \frac{d\sigma_0}{d\Omega_{cm}}(x_- x_+ s, \vartheta_{cm}) \Theta(cuts) , \quad (1)$$

which is based on the factorization theorems of universal infrared and collinear singularities. In the previous formula, $d\sigma_0/d\Omega$ represents the Born-like differential cross section for the process under consideration and $D(x, Q^2)$ are the electron structure functions (SF) for initial and final state radiation. They describe the effects of multiple emission of soft and hard photons in the collinear limit to all orders of perturbation theory. The SF is the solution of the QED Dokshitzer-Gribov-Lipatov-Altarelli-Parisi (DGLAP) evolution equation [3] in the non-singlet channel

$$Q^2 \frac{\partial}{\partial Q^2} D(x, Q^2) = \frac{\alpha}{2\pi} \int_x^1 \frac{dy}{y} P_+(y) D\left(\frac{x}{y}, Q^2\right) , \quad (2)$$

where $P_+(x)$ is the regularized $e \rightarrow e + \gamma$ splitting function. The electron SF has a clear and intuitive meaning: it represents the probability density of finding “inside” a parent electron an electron with momentum fraction x and virtuality Q^2 .

In the literature (see for example [4] and references therein) several solutions of DGLAP equation are available, but we focus our attention on its Monte Carlo solution, known as the Parton Shower algorithm [5–7]. The advantages of the PS are mainly two: it is an *exact* numerical solution of the DGLAP equation and it allows an approximate generation of the photons momenta. The steps of the algorithm can be extracted introducing the Sudakov form factor [8] and, using it, getting an iterative solution of DGLAP equation. Namely, the solution is (here $Q^2 = s$ is understood)

$$\begin{aligned} D(x, s) = & \Pi(s, m^2) \delta(1 - x) + \\ & + \int_{m^2}^s \Pi(s, s') \frac{ds'}{s'} \Pi(s', m^2) \frac{\alpha}{2\pi} \int_0^{x_+} dy P(y) \delta(x - y) + \\ & + \int_{m^2}^s \Pi(s, s') \frac{ds'}{s'} \int_{m^2}^{s'} \Pi(s', s'') \frac{ds''}{s''} \Pi(s'', m^2) \times \\ & \left(\frac{\alpha}{2\pi} \right)^2 \int_0^{x_+} dx_1 \int_0^{x_+} dx_2 P(x_1) P(x_2) \delta(x - x_1 x_2) + \left(\frac{\alpha}{2\pi} \right)^3 \dots \quad (3) \end{aligned}$$

where $\Pi(s_1, s_2) = \exp[-\alpha/2\pi \int_{s_2}^{s_1} ds'/s' \int_0^{x_+} dz P(z)]$ is the Sudakov form factor, which represents the probability that the electron evolves from virtuality s_2 to virtuality s_1 with no emission of photons of energy fraction greater than (an infrared regulator) $\epsilon = 1 - x_+$. Note that the eq. (3) accounts for soft + virtual and real photons radiation up to all order of perturbation theory, in the leading logarithmic approximation.

For the steps of our implementation of the PS algorithm, we refer to [1]. For the scope of this paper, it is sufficient to notice that the algorithm simulates a shower of photons emitted by the electron following the solution of eq. (3). When the algorithm stops, we are left with the energy fraction z_i of each photon (distributed according to the Altarelli-Parisi splitting function), the virtualities of the electron at each branching and the remaining energy fraction x of the electron after the showering. The x variable is distributed according to $D(x, Q^2)$. By means of these quantities, an approximate branching kinematics can be obtained, as discussed below.

For testing purposes, an up to $\mathcal{O}(\alpha)$ PS algorithm has been developed as well. It allows to calculate the corrected cross section of eq. (1) up to $\mathcal{O}(\alpha)$. Such a calculation is strongly required for fully consistent comparisons between the PS predictions and the exact $\mathcal{O}(\alpha)$ ones, in order to keep under control the approximations intrinsic into the PS approach and its theoretical accuracy. The steps required for the $\mathcal{O}(\alpha)$ PS, which are described in [1], can be obtained by using eq. (3) and expanding up to $\mathcal{O}(\alpha)$ the product $D(x_-, Q^2)D(x_+, Q^2)D(y_+, Q^2)D(y_-, Q^2)$ present in eq. (1).

3 Branching kinematics

The main advantage of the PS algorithm with respect to the collinear treatment of the electron evolution is the possibility of going beyond the strictly collinear approximation and generating transverse momentum p_\perp of electrons and photons at each branching. In fact, the kinematics of the branching process $e(p) \rightarrow e'(p') + \gamma(q)$ can be written as

$$p = (E, \vec{0}, p_z) \quad , \quad p' = (zE, \vec{p}_\perp, p'_z) \quad , \quad q = ((1-z)E, -\vec{p}_\perp, q_z) \quad . \quad (4)$$

Once the variables p^2 , p'^2 and z are generated by the PS algorithm, the on-shell condition $q^2 = 0$, together with the longitudinal momentum conservation, allows to obtain an expression for the p_\perp variable:

$$p_\perp^2 = (1-z)(zp^2 - p'^2) \quad (5)$$

at first order in $p^2/E^2 \ll 1$, $p_\perp^2/E^2 \ll 1$. From now on, we will refer to eq. (5) as the “PS prescription”.

Some misbehaviours are connected with this PS picture. First of all, since within the PS algorithm the generation of p'^2 and z are independent, it can happen that in some branching the p_\perp^2 as given by eq. (5) is negative. In order to avoid this problem, the introduction of any kinematical cut on p^2 or z generation (or the regeneration of the whole event) would mean a not correct reconstruction of the SF x distribution, which is important for a precise cross section calculation. Furthermore, in the PS scheme, each fermion produces its photons cascade independently from the other ones, missing the effects due to the interference of radiation coming from different charged particles. As far as inclusive cross sections are considered, these effects are integrated out and we do not expect them to be large, but when exclusive photon variables distributions are looked at, they may be important.

Concerning the first problem, it can be overcome leaving away from a pure PS picture. For example, we can choose to extract the photon $\cos \vartheta_\gamma$ according to the universal leading poles $1/p \cdot k$ present in the matrix element for photon emission (in the following referred to as the “LL prescription”). Namely, we can generate $\cos \vartheta_\gamma$ as

$$\cos \vartheta_\gamma \propto \frac{1}{1 - \beta \cos \vartheta_\gamma} , \quad (6)$$

where β is the speed of the emitting particle. In this way, photon energy and angle are generated independently, differently from eq. (5). The nice feature of this prescription is that $p_\perp^2 = E_\gamma^2 \sin^2 \vartheta_\gamma$ is always well defined and the x distribution reproduces exactly the SF, because we do not need to impose further kinematical cuts to avoid unphysical events. At this stage, the PS is used only to generate photons energies and photons multiplicity. The problem of including the radiation interference is still unsolved, because the variables of photons emitted by a fermion are still not correlated to the other charged particles. The phenomenological comparison between PS and LL prescriptions will be shown in the next section.

The issue of including photon interference can be successfully worked out looking at the Yennie-Frautschi-Suura (YFS) formula [9,10]:

$$d\sigma_n \approx d\sigma_0 \frac{e^{2n}}{n!} \prod_{l=1}^n \frac{d^3 \mathbf{k}_l}{(2\pi)^3 2k_l^0} \sum_{i,j=1}^N \eta_i \eta_j \frac{-p_i \cdot p_j}{(p_i \cdot k_l)(p_j \cdot k_l)} . \quad (7)$$

It is a very general formula which gives the differential cross section $d\sigma_n$ for the emission of n photons, whose momenta are k_1, \dots, k_n , from a kernel process described by $d\sigma_0$ and involving N fermions, whose momenta are p_1, \dots, p_N . In eq. (7), η_i is a charge factor, which is $+1$ for incoming e^- or outgoing e^+ and -1 for incoming e^+ or outgoing e^- . Note that eq. (7) is valid in the soft limit ($k_i \rightarrow 0$). The important point is that it also accounts for coherence effects. From YFS formula, it is straightforward to read out the angular spectrum of

the l^{th} photon (“YFS prescription”):

$$\cos \vartheta_l \propto - \sum_{i,j=1}^N \eta_i \eta_j \frac{1 - \beta_i \beta_j \cos \vartheta_{ij}}{(1 - \beta_i \cos \vartheta_{il})(1 - \beta_j \cos \vartheta_{jl})} . \quad (8)$$

It is worth noticing that in the LL prescription, the same quantity writes as

$$\cos \vartheta_l \propto \sum_{i=1}^N \frac{1}{1 - \beta_i \cos \vartheta_{il}} \quad (9)$$

whose terms are of course contained in eq. (8).

In order to consider also coherence effects in the angular distribution of the photons, we may generate $\cos \vartheta_\gamma$ according to eq. (8), rather than eq. (9). We expect that the improvements on photon angular distribution will be sizeable, as discussed in the next section.

4 Comparisons and results

In this section, we deal with the application of the PS, mainly in its $\mathcal{O}(\alpha)$ realization, to the Bhabha process at large angle, as implemented in BABAYAGA. To test the theoretical accuracy of the PS approach in total cross section calculation as well as in event generation, an exact $\mathcal{O}(\alpha)$ calculation has been carried out in the program LABSPV, used as a benchmark calculation. The code is described in [1,11] and it is based on the formulae given in [12,13].

As first comparison, we consider the results of PS and LL prescriptions on photon distributions. They are obtained by means of the PS algorithm truncated at $\mathcal{O}(\alpha)$. We generated a sample of radiative Bhabha events at a typical DAΦNE energy ($\sqrt{s} = M_\Phi$) and requiring the final state e^+ and e^- to lie within 20° and 160° , with at least 0.4 GeV of energy and a maximum acollinearity between them of 10° . Furthermore, we require that the photon has at least 10 MeV of energy. For those unphysical $p_\perp^2 < 0$ events generated in the pure PS prescription, we arranged to set the photon collinear to the emitting particle ($p_\perp^2 = 0$), without regenerating the event. In fig. 1, the energy and angular distributions of the photon are plotted. We note that, except some details, the two angular generation schemes give roughly the same answer: this is consistent with the PS picture, based on the leading logarithmic treatment of the branching kinematics.

Next, we consider how the distributions change if we weight photon angle by eq. (8) and we compare the results to the exact $\mathcal{O}(\alpha)$ distributions. On the left, fig. 2 shows the angular distribution of the photon, imposing the same

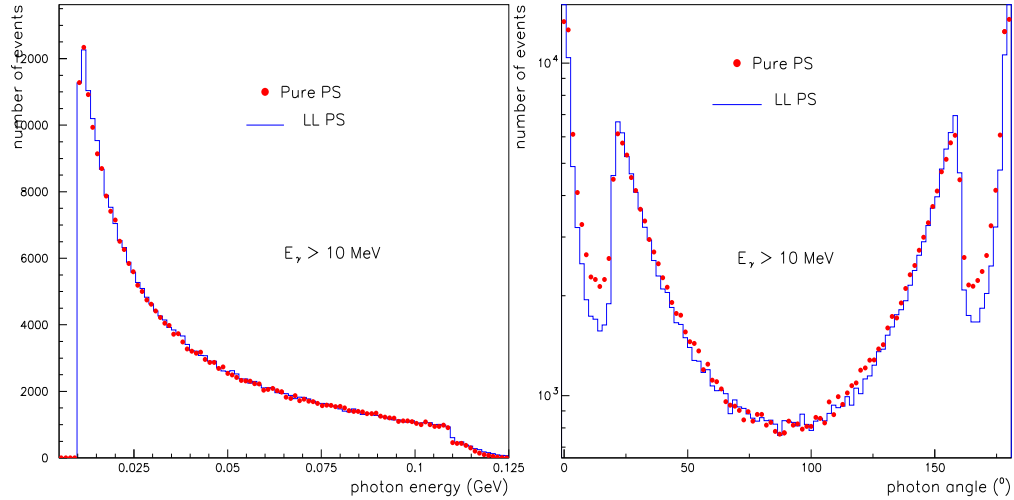


Fig. 1. Comparison of energetic (on the left) and angular (on the right) photon spectrum given by $\mathcal{O}(\alpha)$ PS with PS and LL prescription for photon p_\perp generation.

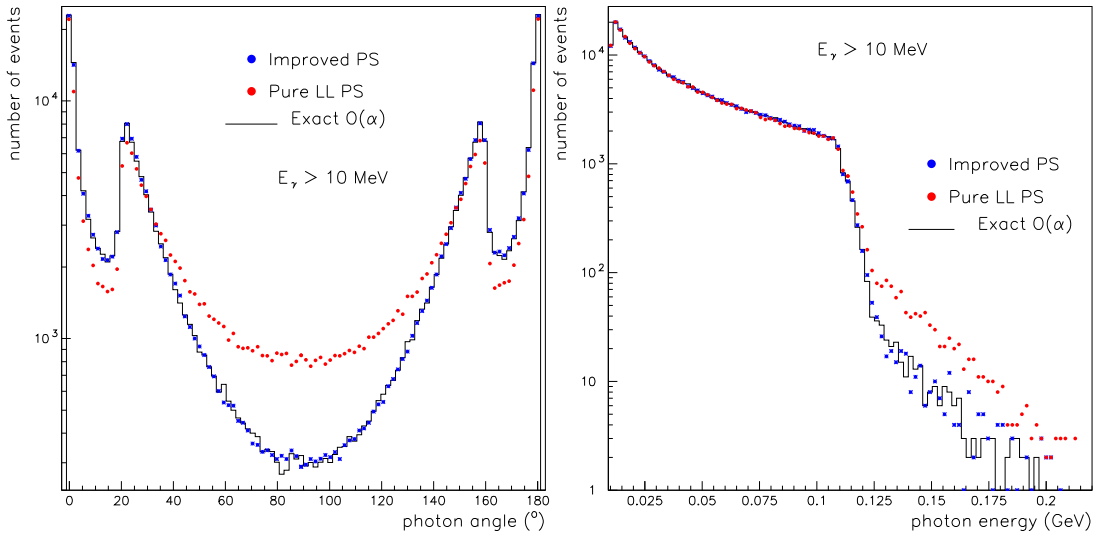


Fig. 2. Comparison of the angular (on the left) and energetic (on the right) photon spectra obtained from LL and YFS prescriptions and exact $\mathcal{O}(\alpha)$ matrix element.

event selection criteria of the previous plots: the red dots represent the LL prescription, the blue ones the YFS prescription and the solid histogram is the exact $\mathcal{O}(\alpha)$ distribution. The improvement due to the inclusion of radiation coherence by means of YFS formula is evident: the YFS-PS spectrum fits perfectly to the exact $\mathcal{O}(\alpha)$ one. On the right, the photon energy distributions are compared: we note that the result of LL description is very good by itself (except close to the distribution end, where anyway the statistics is very poor), as a consequence of the good approximation of the Altarelli-Parisi splitting function to reproduce the correct energy spectrum. Nevertheless, the YFS-PS

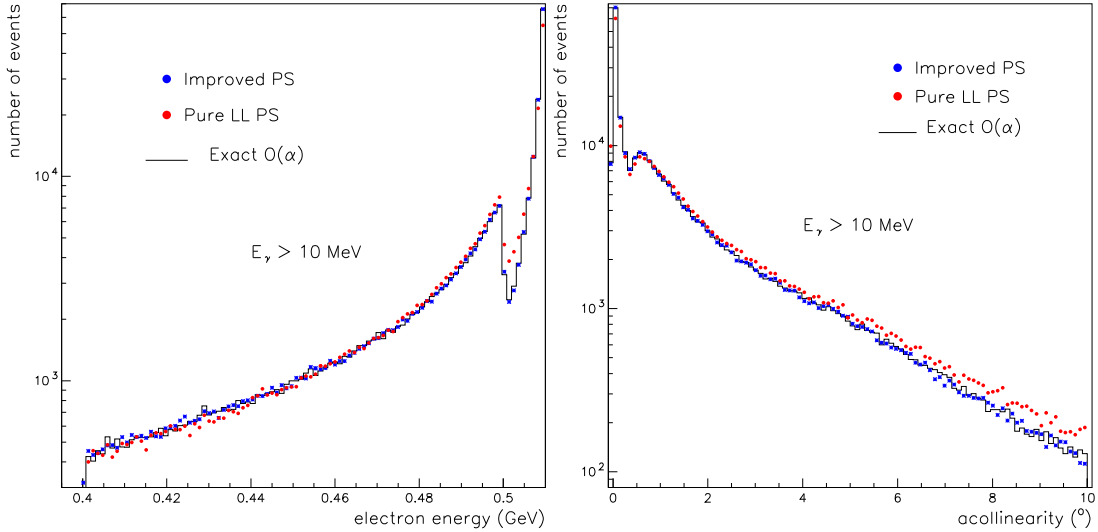


Fig. 3. Comparison of electron energy (on the left) and acollinearity (on the right) distributions obtained from LL and YFS prescriptions and exact $\mathcal{O}(\alpha)$ matrix element.

fits better to the exact distribution, even at its end. The same comments apply to fig. 3, where variables referring to final state fermions are plotted for the same sample of events: electron energy (on the left) and acollinearity (on the right) distributions are shown.

Up to now, we presented the results of the $\mathcal{O}(\alpha)$ PS, but the YFS prescription of eq. (8) has been applied to the all orders PS as well. As an example, we considered a sample of Bhabha events generated by means of the PS to all orders, imposing the same cuts as before and requiring that the most energetic photon of each event has at least 10 MeV of energy. The differences (due to coherence) on the angular distribution of the most energetic photon as given by the LL PS and the YFS PS are evident in fig. 4 (on the left). In the same figure, on the right, the effects of higher order photon emission are shown. The distribution of the energy lost because of radiation is plotted, comparing the $\mathcal{O}(\alpha)$ and the up to all order PS distribution. In this case, no cut is applied to the photon(s).

Finally, we give an estimate of the theoretical accuracy of the PS approach in inclusive cross section calculation. The bulk of the terms missed in the PS scheme in its all orders implementation can be estimated, up to very negligible uncertainty at next to leading $\mathcal{O}(\alpha^2)$ level [1], by means of the relative difference between the exact $\mathcal{O}(\alpha)$ corrected cross section and the $\mathcal{O}(\alpha)$ PS one. In figure (5), such a difference is plotted, as a function of the acollinearity cut, for inclusive Bhabha cross section at $\sqrt{s} = M_\Phi$, requiring the final state e^+ and e^- to have at least 0.4 GeV of energy and considering $20^\circ < \vartheta_\pm < 160^\circ$ and $50^\circ < \vartheta_\pm < 130^\circ$ acceptance region. For the “best” prescription, the YFS one,

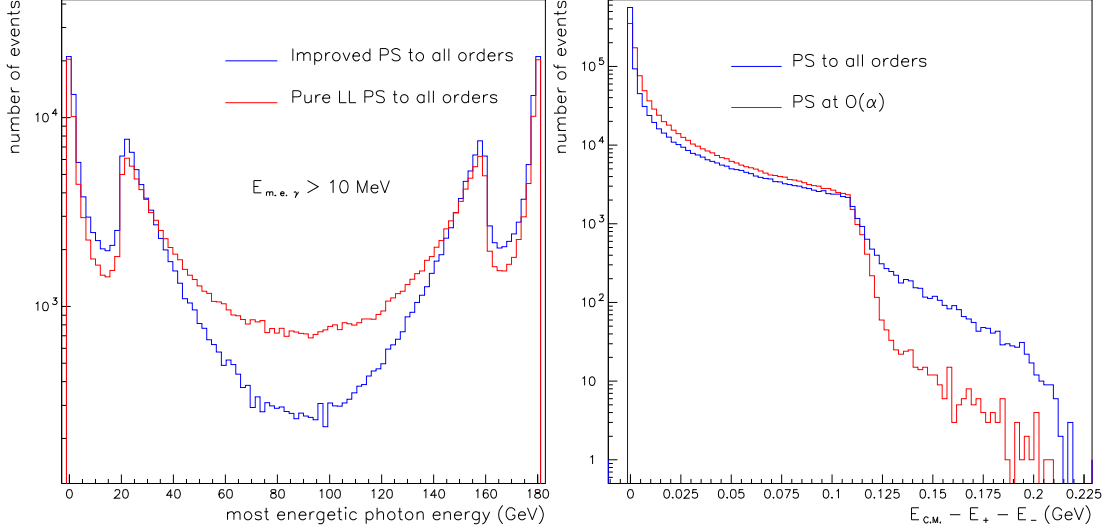


Fig. 4. On the left, the angular distributions of the most energetic photon as obtained with the LL PS and YFS PS to all orders are compared for a sample of radiative Bhabha events. On the right, the radiation energy distributions as obtained with the $\mathcal{O}(\alpha)$ PS and all orders PS are compared for a sample of inclusive Bhabha events.

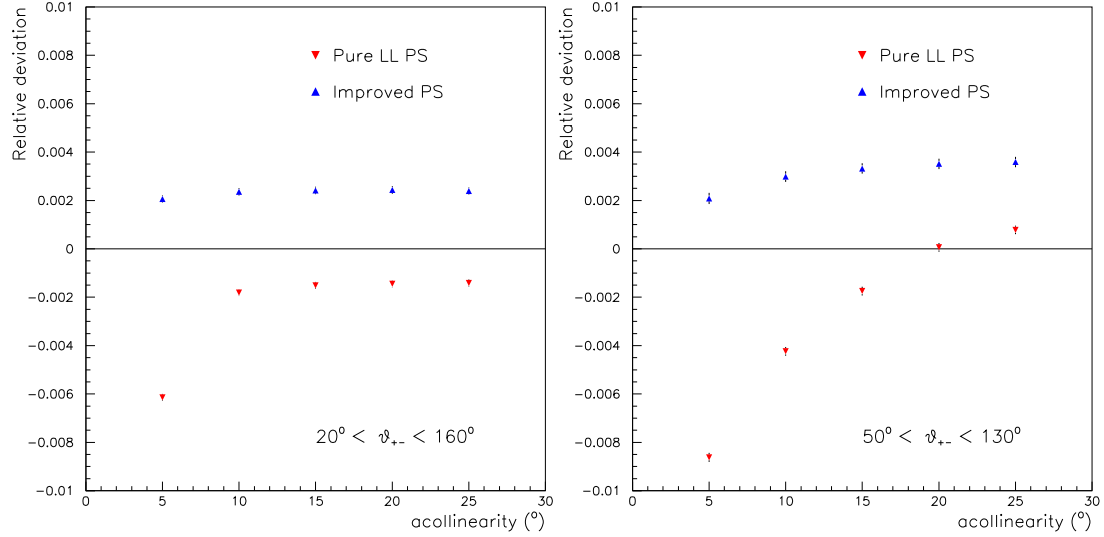


Fig. 5. Relative difference between $\mathcal{O}(\alpha)$ corrected Bhabha cross section at $\sqrt{s} = 1$ GeV, as given by the exact matrix element and the $\mathcal{O}(\alpha)$ PS (in the LL and YFS prescriptions). Two different angular acceptance regions are considered and the difference is plotted as a function of the acollinearity cut.

the amount of $\mathcal{O}(\alpha)$ missing contributions is contained within the 0.4% and they could be further reduced, by an *ad hoc* and tuned choice of the Q^2 scale present in the electron SF. This topic is widely discussed in [1]. It is worth noticing that the exact versus PS difference is less dependent on the acollinearity cut when the YFS-improved PS is considered. The next step toward the

reduction of the theoretical error (and the complete independence from *ad hoc* recipes) would be the real merging of the exact $\mathcal{O}(\alpha)$ matrix element into the PS. Work is in progress in this direction.

5 Conclusions

The QED Parton Shower algorithm has been applied to QED processes event generation at e^+e^- flavour factories, in order to simulate the phenomenologically relevant radiative corrections to all orders of perturbation theory and to provide a useful Monte Carlo event generator (BABAYAGA) for data analysis. The theoretical accuracy of the event generator is estimated to be within the 0.5% level for Bhabha scattering, in typical event selection criteria for data analysis at flavour factories. After a brief sketch of the theoretical framework which the PS algorithm is based on, in this paper the photons kinematics generation is critically revised. We introduced three different schemes for generating photons angles, named the pure PS, the LL and the YFS prescription. In particular, the last one is inspired to the YFS formula [9,10] of eq. (7). By means of an $\mathcal{O}(\alpha)$ PS, the results from the three prescriptions have been systematically compared to the exact $\mathcal{O}(\alpha)$ ones. We pointed out and showed that the YFS-PS has the best behaviour to simulate and generate also radiative events, fitting very well to all the exact $\mathcal{O}(\alpha)$ distributions. The new release of the BABAYAGA event generator is built on this theoretical background. The code is available and can be downloaded from the web site <http://www.pv.infn.it/~nicrosi/programs.html>.

The open issue for the next future is the merging of the exact $\mathcal{O}(\alpha)$ matrix element with the PS, in order to make it independent from *ad hoc* recipes and to actually shift the theoretical uncertainty to the next to leading order α^2 corrections.

6 Acknowledgments

My work is done in collaboration with Guido Montagna, Oreste Nicrosini and Fulvio Piccinini, whom I wish to thank for their constant support to my work. I'm grateful also to Achim Denig, of the KLOE Collaboration, for his interest in our work and very useful discussions. Finally, I thank the INFN, Sezione di Pavia, for the use of the computer facilities. The author acknowledges partial support from the EEC-TMR Program, Contract N. CT98-0169.

References

- [1] C. M. Carloni Calame, C. Lunardini, G. Montagna, O. Nicrosini and F. Piccinini, *Nucl. Phys.* **B 584** (2000) 459-479.
- [2] See, for example, G. Montagna, O. Nicrosini and F. Piccinini, *Phys. Rev. D* **48** (1993) 1021 and references therein.
- [3] V.N. Gribov and L.N. Lipatov, *Sov. J. Nucl. Phys.* **15** (1972) 298; G. Altarelli and G. Parisi, *Nucl. Phys.* **B 126** (1977) 298; Y.L. Dokshitzer, *Sov. Phys. JETP* **46** (1977) 641.
- [4] G. Montagna, O. Nicrosini and F. Piccinini, *Riv. Nuovo Cim.*, Vol. **21** (1998) 1, [hep-ph/9802302](#).
- [5] R. Odorico, *Nucl. Phys.* **B 172** (1980) 157, *Phys. Lett.* **B 102** (1981) 341; P. Mazzanti and R. Odorico, *Phys. Lett.* **B 95** (1980) 133; G. Marchesini and B.R. Webber, *Nucl. Phys.* **B 238** (1984) 1; T. Sjöstrand, *Phys. Lett.* **B 310** (1985) 321; K. Kato and T. Munehisa, *Phys. Rev. D* **39** (1989) 156; K. Kato, T. Munehisa and H. Tanaka, *Z. Physik C* **54** (1992) 397. A review of the PS method in QCD and relative QCD event generators can be found in: R.K. Ellis, W.J. Stirling and B.R. Webber, *QCD and Collider Physics*, Cambridge University Press.
- [6] J. Fujimoto, T. Munehisa and Y. Shimizu, *Prog. Theor. Phys.* **90** (1993) 177; Y. Kurihara, J. Fujimoto, T. Munehisa and Y. Shimizu, *Prog. Theor. Phys.* **96** (1996) 1223, *ibid.* **95** (1996) 375.
- [7] H. Anlauf et al., *Comput. Phys. Commun.* **70** (1992) 97.
- [8] V.V. Sudakov, *Sov. Phys. JETP* **3** (1956) 65.
- [9] D. R. Yennie, S. C. Frautschi and H. Suura, *Ann. Phys.* **13** (1961) 379.
- [10] T. Muta, *Foundations of Quantum Chromodynamics*, second edition, World Scientific, 2000.
- [11] M. Cacciari, G. Montagna, O. Nicrosini and F. Piccinini, in *Report of the Working Group on Precision Calculations for the Z Resonance*, D. Bardin, W. Hollik, G. Passarino eds., CERN Report **95-03** (CERN, Geneva, 1995), p. 389, *Comput. Phys. Commun.* **90** (1995) 301.
- [12] M. Caffo, E. Remiddi et al., “Bhabha Scattering”, in *Z Physics at LEP1*, G. Altarelli, R. Kleiss and C. Verzegnassi eds., CERN Report **89-08** (CERN, Geneva, 1989), Vol. 1, p.171; M. Greco, *Riv. Nuovo Cim.*, Vol. **11** (1988) 1.
- [13] F.A. Berends et al., *Nucl. Phys.* **B 202** (1981) 63.